LEVEL ESTIMATION FOR SPARSE RECONSTRUCTION IN DISCRETE TOMOGRAPHY

Yen-ting Lin, Antonio Ortega and Alexandros G. Dimakis

Department of Electrical Engineering-Systems
University of Southern California
Los Angeles, California, 90089-2564, U.S.A

ABSTRACT

In discrete tomography (DT), the goal is to reconstruct from multiple linear projections an unknown image, which is known to have few distinct pixel level intensities. Such images arise in tomography problems where very high contrast is expected, e.g., in angiography medical imaging. A common assumption for DT is that the set of possible intensity levels is known in advance. However, determining the intensity levels is a difficult problem, coupled with measurement calibration and the used reconstruction algorithm. We introduce an unsupervised DT algorithm that jointly reconstructs the image and estimates the unknown intensity levels. Our algorithm alternates between (i) an l_1 sparse recovery step with a reweighed cost function that pushes the reconstructed values close to the estimated intensities, and (ii) an estimation step for the most likely intensity levels. We experimentally demonstrate that the proposed algorithm successfully estimates the unknown levels and leads to high quality reconstruction of angiographic images.

Index Terms— gray level estimation, sparse reconstruction, discrete tomography

1. INTRODUCTION

In computed tomography the goal is to reconstruct an interior image from a series of linear projections on the boundary. In this paper we address the problem of reconstructing an image which has only few different pixel intensity levels. This scenario can happen in tomography problems where the very high contrast is expected, e.g., in medical imaging applications such as angiography. Moreover, forcing the reconstructed pixels to belong tofew discrete levels also has a De-noising effect and can be more generally useful. And it is also desirable to reduce the number of projection angles in order to limit the radiation exposure. Based on these two ideas, we are interested in reconstructing an image with a few pixel levels from a small set of projections, i.e., we are considering a *Discrete Tomography* (DT) problem [1]. There has been substantial prior work on DT reconstruction algorithms. Fishburn *et al.* [2] and Weber *et al.* [3] used linear programming (LP) relaxation techniques to approximate DT using convex optimization. Batenburg *et al.* proposed a discrete algebraic reconstruction algorithm to iteratively update the object boundary and reported some success in electron tomography datasets [4, 5]. Liao and Herman [6] considered a statistical reconstruction method with more than two gray levels based on Gibbs priors. For a comprehensive review, we refer to Herman and Kuba [1] and references therein.

A common assumption for the above algorithms is that the set of possible intensity levels is known in advance. However, in practice determining the intensity levels is very challenging and coupled with other aspects of the problem, such as measurement calibration and the specific reconstruction algorithm chosen. For example, in angiography only two types of regions need to be considered: blood vessels enhanced by a radio-opaque contrast agent and the "background", which represents the rest of body [7]. The target image will be very high-contrast, but the intensity levels of blood vessels are very hard to determine *a priori* since they are related to the blood flow and the chosen contrast agent [8].

To the best of our knowledge, only very few literatures explicitly address the *unknown intensity discrete tomography problem*. Batenburg *et al.*[9] proposed a semi-automatic algorithm for intensity level estimation, which requires the user to select manually regions that are expected to belong to the same gray level. Lukić[10] combined the multi-well potential function into the object function to encourage the solution staying on gray level values, but it's not an easy task to design the potential function without trapping the the solution in the local minimum. In contrast, in this paper we introduce a *completely unsupervised* discrete tomography algorithm that jointly reconstructs the image and estimates the unknown intensity levels.

We build on our prior work [11], which addressed the binary DT problem for known intensity levels. In that work, we introduced the step-function dictionary to efficiently represent a binary image and used the L_1 reweighing of Candes *et al.* [12], combined with bounding the values in $[0, 1]$ to obtain a reconstruction algorithm that encourages the solution to come closer to the boundary points $\{0, 1\}$, thus leading to

This work is supported in part by Chevron Corp. under the joint project Center for Interactive Smart Oilfield Technologies (CiSoft), at the University of Southern California.

a two-level image. In this paper we extend this algorithm by (i) adding a level-estimation step within each iteration and (ii) allowing the superposition of multiple levels.

For the ideal reconstructed discrete image, the histogram of pixel intensity levels should only have a few peaks. Thus, our proposed level-estimation step is essentially a clustering algorithm on the histogram of reconstructed image. Subsequently, the estimated levels are used as an input in the next reweighed l_1 step. Our preliminary simulation results show that the proposed algorithm successfully estimates the discrete intensity levels and accurately reconstructs the images from a small number of linear projections. Since we expect noise in the measurements, we use l_1-norm optimization with a bounded l_2 measurement error constraint, the well-known LASSO [13, 14] method.

The remainder of the paper is organized as follows. In Section 2 we formulate the unknown level discrete tomography problem. Section 3 gives an overview and provides some intuition about our proposed approach for intensity level estimation. Simulated reconstruction results and discussions are presented in Section 4. Section 5 concludes this paper and points out some future directions.

2. PROBLEM FORMULATION

We assume a $M+1$ level signal which only takes values in $\{0, k^1, \ldots, k^M\}$, where k^λ is an unknown positive number. Let $f(\alpha, \beta)$ be a 2D image and let the measurements be parallel projections along different angles. The relationship between the projection measurements and image f can be modeled using the 2D discrete Radon transform [15]. Each projection is the sum of all pixels a given ray is passing through, with trigonometric interpolation being used for the non-grid points. If the image has $p \times q$ pixels, we can reshape the $2D$ image f into a $1D$ vector $\mathbf{x}$ with dimension $n = p \cdot q$. For each projection angle, equally pixel-length spaced measurements are sampled. If we take γ sample points for each projection angle, the measured data for one specific angle will be a dimension γ vector $\mathbf{p}$. Then we can write the projection operator in matrix form:

$$\mathbf{W}_\theta \mathbf{x} = \mathbf{p}_\theta, \tag{1}$$

where $\mathbf{W}_\theta$ is a $\gamma \times n$ line projection matrix with angle θ. If we have d different viewing angles, we can represent the projection matrices and measurements as:

$$\mathbf{A}\mathbf{x} = \mathbf{y}, \tag{2}$$

with

$$\mathbf{A} = \begin{bmatrix} \mathbf{W}_{\theta_1} \\ \vdots \\ \mathbf{W}_{\theta_d} \end{bmatrix}, \quad \mathbf{y} = \begin{bmatrix} \mathbf{p}_{\theta_1} \\ \vdots \\ \mathbf{p}_{\theta_d} \end{bmatrix} \tag{3}$$

$\mathbf{A}$ will be an $m \times n$ line projection matrix that maps $\mathbf{x}$ onto measurement data $\mathbf{y}$, where $m = \gamma \cdot d$.

The reconstruction problem is, given the projection matrix $\mathbf{A}$ and data $\mathbf{y}$, with $m << n$, to find a discrete solution $\mathbf{x}$, $x_i \in \{0, k^1, \ldots, k^M\}$. This is an inverse problem with the solution having $M+1$ unknown intensity levels. We assume the maximum value of $k^\lambda,\ \lambda = 1, \ldots, M$ is bounded by S, $0 \le k^\lambda \le S$.

3. ALGORITHM

We propose an iterative linear programming relaxation algorithm to handle this problem. Based on our previous work [11] on binary tomography, a step-function basis $\mathbf{T}$ was introduced. We extend this concept to represent a $M+1$ level discrete image $\mathbf{x}$ as the linear combination of several two-level signals with coefficients $\left[\mathbf{u}^1, \mathbf{u}^2, \ldots \mathbf{u}^M\right]$

$$\mathbf{x} = \sum_{\lambda=1}^{M} k^\lambda \cdot \mathbf{T}\mathbf{u}^\lambda, \ \ u_i^\lambda \in \{-1, 0, 1\} \tag{4}$$

It leads the reconstruction algorithm to be an reweighed l_1 norm convex programming formulation that favors the sparseness of $\mathbf{u}^\lambda$

$$\left[\mathbf{u}^1, \ldots, \mathbf{u}^M\right] \ = \arg\min_{\mathbf{u}^\lambda} \sum_{\lambda=1}^{M} \left\| \mathbf{w}^\lambda . * \mathbf{u}^\lambda \right\|_1 \tag{5}$$

$$\text{subject to} \qquad \mathbf{y} = \mathbf{A}\mathbf{x} \tag{6}$$

$$\mathbf{x} = \sum_{\lambda=1}^{M} \widetilde{k}^\lambda \cdot \mathbf{T}\mathbf{u}^\lambda \tag{7}$$

$$-\mathbf{1} \le \mathbf{u}^\lambda \le \mathbf{1}, \ \ 0 \le \mathbf{x}_i \le D(i) \tag{8}$$

There are two major questions in our algorithm: how to get the intensity estimate $\widetilde{k}^\lambda$ and the boundary of feasible region $D(i)$? The intensity estimate $\widetilde{k}^\lambda$ is critical to the reconstruction result. With the intensity estimate $\widetilde{k}^\lambda$, the reweighed algorithm tends push the coefficient u_i^λ into the boundary $u_i^\lambda \in [-1, 1]$ which means $u_i^\lambda \in \{-1, 0, 1\}$. This leads to a solution $\mathbf{x}$ where every pixel has a discrete intensity level: $x_i \in \{0, \widetilde{k}^1, \ldots, \widetilde{k}^M\}$. The size of feasible region also plays an important role for the reweighed l_1 minimization procedure. For example, assume some pixels x_i have the intensity level k^λ, and we select a larger feasible region for them, say, $D(i) > k^\lambda$. Because all the entries of the projection matrix $\mathbf{A}$ are non-negative and reweighed l_1 tends to push the solution towards the range boundaries, we will have some $x_j = D(i)$ and some $x_l \le k^\lambda$ in order to satisfy $\mathbf{A}\mathbf{x} = \mathbf{y}$. The histogram of the reconstructed image will spread out over the region. On the other hand, if we set the feasible region too small, $D(i) < k^\lambda$, no solution can be found for $\mathbf{A}\mathbf{x} = \mathbf{y}$ inside the feasible region $0 \le x_i \le D(i)$.

We initialize our algorithm by setting the intensity estimate and feasible region with the upper bound, $\widetilde{k}^\lambda = S, \ 0 \le$

$x_i \leq S$, and run the sparse reconstruction algorithm to get an initial solution $\mathbf{x}^0$. Then we update the estimated intensity level $\widetilde{k}^\lambda$. We define a threshold ϵ and form a histogram of the intensities of all pixels with intensities greater ϵ, $\mathbf{x}_i^0 \geq \epsilon$. By using Gaussian Mixture Model (GMM) based clustering [16], we partition this histogram them into M groups. We only use pixel values greater than ϵ for clustering because 0 is a prior known level, whose intensity does not need to be estimated. Furthermore, the Gaussian distribution used in GMM is symmetrical and pixel intensities are non-negative, thus if we performed GMM clustering on all pixel values we would never obtain a cluster with mean 0. In summary, we use simple thresholding to assign small pixel values to the cluster with intensity 0, while using GMM to estimate the remaining intensities from pixel data above the threshold. We update the estimated intensity level $\widetilde{k}^\lambda$ based on the mean c^λ and variance σ^λ of each cluster:

$$\widetilde{k}^\lambda \leftarrow \widetilde{k}^\lambda - \gamma(\frac{1}{\sigma^\lambda}) \cdot (k^\lambda - c^\lambda), \tag{9}$$

The coefficient function $\gamma(\frac{1}{\sigma^\lambda})$ is defined as $\min\{0.25, \frac{1}{\sigma^\lambda}\}$ to control the update speed. The new intensity estimate $\widetilde{k}^\lambda$ is chosen so that it moves closer to the mean c^λ of cluster G_λ.

After updating the intensity estimate $\widetilde{k}^\lambda$, we need to define the new feasible region for the reweighed l_1 minimization. In the previous step, the result for GMM clustering can determine to which cluster each pixel x_i belongs. However, for a pixel intensity which is located near the boundary between two clusters, there is uncertainty about which cluster it actually belongs to. Thus, instead of using the GMM clustering result, we propose a soft decision for the feasible region. We define the 'forward mapping' of each cluster $\mathbf{z} = \widetilde{k}^\lambda \cdot \mathbf{T}\mathbf{u}^\lambda$ and declare pixel i belongs to group λ if $z_i \geq \epsilon$. Note that it is possible that one pixel belongs to several different clusters.

For the ideal case, every pixel only belongs to one cluster and the intensity $\widetilde{k}^\lambda$ gives the gray level of this cluster. The feasible region for the pixel i in cluster G_λ will be $0 \leq x_i \leq \widetilde{k}^\lambda$. But in case that a pixel x_j belongs to several different clusters $\lambda_1, \ldots, \lambda_p$, we choose the boundary for x_j as $0 \leq x_j \leq \max_{\lambda_1,\ldots,\lambda_p} \widetilde{k}^\lambda$. By choosing a larger feasible region, we make sure that at least there will be a solution for the convex programming.

When we have a perfect estimate of the intensity level, $\widetilde{k}^\lambda = k^\lambda$, in other words we have the exact feasible region $0 \leq x_i \leq k^\lambda$, this problem is reduced to the binary tomography problem we addressed in our previous work.

4. SIMULATION RESULTS

In the first simulation, we use a 64×64 simplified Shepp-Logan phantom with three intensity levels as the testing image. The intensity for the outer circle is 80, and for the right and lobes is 16. For the measurements, $\{12, 18\}$ different projection angles are taken uniformly between $[0, 180]$ and zero mean Gaussian noise is added with variance $\sigma = \{0, 0.1, 0.2, 0.5, 1, 2, 5\}$. We set the upper bound $D = 100$ and use CVX [17] as our convex programming solver.

We show the histogram of the reconstructed image through iterations in Figure 1. After we update the intensity level, the distribution of histogram becomes more concentrated and finally converges to a few peaks. From the results, we see that most of the non-zero entries x_i stay on the boundary of feasible region as we expected. The mean square error of the reconstructed image with different noise variance and number of projections is shown in Figure 2. We compare the results with the standard filter-back projection[18], and total variation(TV) reconstruction[19]. It shows our method has much better performance than the other two approaches and it outperforms the TV method even with fewer measurements. Compared to our previous work, even though not knowing the intensity level as a prior information increases the difficulty of this problem, the overall results still show good performance.

In the second experiment, we use a testing image with size 256×256. When we solve the large dimension convex programming problem, the conventional second order method, e.g., interior point method requires huge memory space to store the Hessian matrix. Instead, we use the first order algorithm, Projected Gradient[20] method to solve it with limited memory requirement. The convex problem can be summarized with two constraints

$$\begin{aligned} \text{Min} \quad & \sum_\lambda \|\mathbf{W}_\lambda \mathbf{u}_\lambda\|_1 \\ \text{Subject to} \quad & C_{1:\text{Data fitting}} : \mathbf{A}(\sum_\lambda \widetilde{k_\lambda} \cdot \mathbf{D}\mathbf{u}_\lambda) = \mathbf{y} \\ & C_{2:\text{Boundary}} : LB(i) \leq \mathbf{T}(\mathbf{u})_i \leq UB(i) \end{aligned}$$

The Projected Gradient algorithm will project the solution and gradient onto feasible sets. But finding the intersection of $C = C_1 \cap C_2$ is not an easy task. Instead, we alternately solve these two problems(See figure 3)

$$\begin{aligned} \text{Min} \quad & \textstyle\sum_\lambda \|\mathbf{u}_\lambda\|_1 + \mu \cdot \phi_{Bd}(\mathbf{u}) && (10) \\ \text{Subject to} \quad & \mathbf{u} \in C_{1:\text{Data fitting}} && (11) \end{aligned}$$

$$\begin{aligned} \text{Min} \quad & \textstyle\sum_\lambda \|\mathbf{u}_\lambda\|_1 + \nu \cdot \|\mathbf{A}\mathbf{x} - \mathbf{b}\|_2 && (12) \\ \text{Subject to} \quad & \mathbf{u} \in C_{2:\text{Boundary}} && (13) \end{aligned}$$

The result is shown in figure 4. After projected on data fitting set, some pixels may become negative4. Next step it will be projected onto the boundary set and move to our preferred solution. The change of MSE with iterations is listed in 5.

5. CONCLUSION

We have presented a new automatic intensity level estimation algorithm for discrete tomography, which focuses on recon-

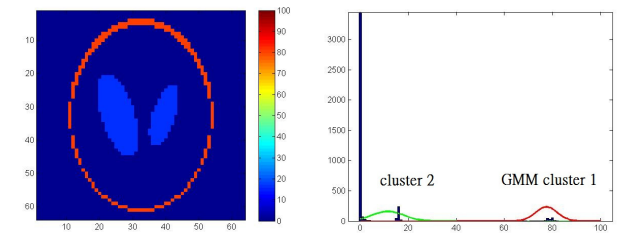

(a) Testing phantom (b) After 1 iteration

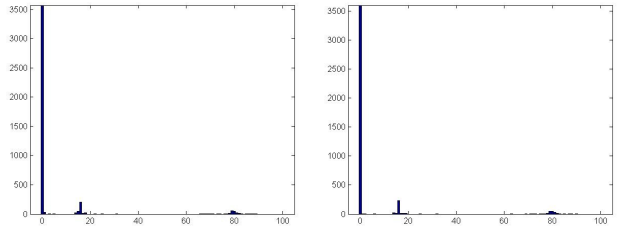

(c) After 2 iterations (c) After 3 iterations

Fig. 1. Shepp-Logan phantom and histogram of the reconstructed image

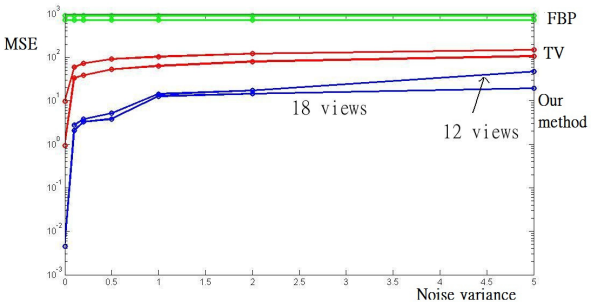

Fig. 2. MSE vs Noise level. Blue: Our method, Red: Total variation, Green: FBP

struction of unknown discrete level images that have a sparse representation under certain dictionary. Our algorithm iterates between reweighed l_1 minimization and GMM histogram clustering steps to estimate the unknown intensity levels. The proposed algorithm had very good performance in our preliminary experimental evaluations. It outperforms the conventional TV method even with fewer measurements. Future work involves understanding the performance of the proposed algorithm under different noise and image models, for example using Poisson models for the noise statistics of the X-ray detector. And we plan to develop an method on the top of our current work to handle the unknown number of intensity level case.

We are currently using CVX as our convex programming solver which limits the image size by 100×100 on a typical PC. For large image, we use Projected Gradient method to

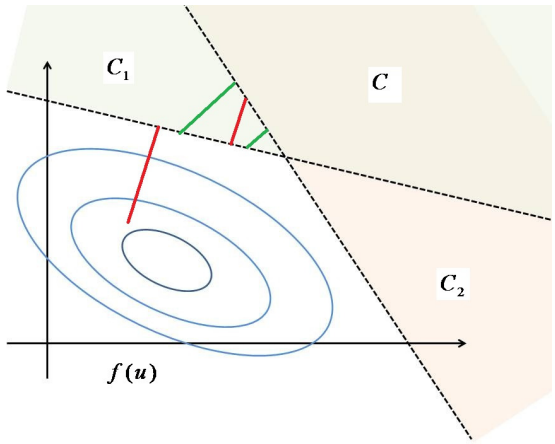

Fig. 3. Alternating projection on two convex sets

handle the problem. But it suffers from the slow convergence speed. In future work we will explore the convergence behavior of such first order algorithms to work on high resolution images.

References

[1] G.T. Herman and A. Kuba, *Discrete Tomography: Foundations, Algorithms, and Applications*, Birkhauser, 1999.

[2] P. Fishburn, P. Schwander, L. Shepp, and RJ Vanderbei, "The discrete Radon transform and its approximate inversion via linear programming," *Discrete Applied Mathematics*, vol. 75, no. 1, pp. 39–61, 1997.

[3] S. Weber, C. Schnorr, T. Schule, and J. Hornegger, "Binary tomography by iterating linear programs," *COMPUTATIONAL IMAGING AND VISION*, vol. 31, pp. 183, 2006.

[4] KJ Batenburg and J. Sijbers, "DART: A fast heuristic algebraic reconstruction algorithm for discrete tomography," in *Proceedings of the IEEE International Conference on Image Processing, San Antonio, Texas*, 2007.

[5] KJ Batenburg, S. Bals, J. Sijbers, C. K
"ubel, PA Midgley, JC Hernandez, U. Kaiser, ER Encina, EA Coronado, and G. Van Tendeloo, "3D imaging of nanomaterials by discrete tomography," *Ultramicroscopy*, vol. 109, no. 6, pp. 730–740, 2009.

[6] H.Y. Liao and G.T. Herman, "A coordinate ascent approach to tomographic reconstruction of label images from a few projections," *Discrete Applied Mathematics*, vol. 151, no. 1-3, pp. 184–197, 2005.

[7] GT Herman and A. Kuba, "Discrete tomography in medical imaging," *Proceedings of the IEEE*, vol. 91, no. 10, pp. 1612–1626, 2003.

[8] F. Cademartiri, N.R. Mollet, A. van der Lugt, E.P. McFadden, T. Stijnen, P.J. de Feyter, and G.P. Krestin, "Intravenous Contrast Material Administration at Helical 16–Detector Row CT Coronary Angiography: Effect of Iodine Concentration on Vascular Attenuation1," *Radiology*, vol. 236, no. 2, pp. 661, 2005.

[9] KJ Batenburg, W. van Aarle, and J. Sijbers, "A Semi-Automatic Algorithm for Grey Level Estimation in Tomography," *Pattern Recognition Letters*, 2010.

[10] T. Lukić, "Discrete tomography reconstruction based on the multi-well potential," *Combinatorial Image Analysis*, pp. 335–345, 2011.

[11] Y.T. Lin, A. Ortega, and A.G. Dimakis, "Sparse Recovery for Discrete Tomography," in *Prof. of ICIP 2010*, Hong Kong, Sept. 2010.

[12] E.J. Candes, M.B. Wakin, and S.P. Boyd, "Enhancing sparsity by reweighted l 1 minimization," *Journal of Fourier Analysis and Applications*, vol. 14, no. 5, pp. 877–905, 2008.

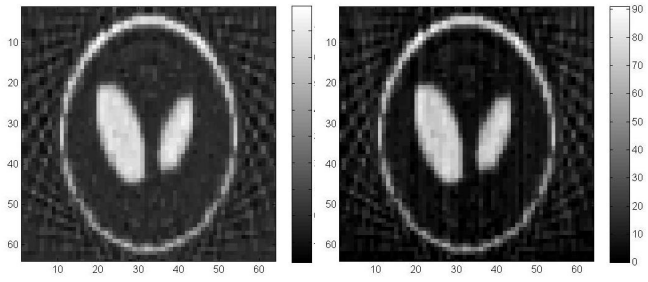

(a) Projected on data fitting (b) Projected on boundary

Fig. 4. Result for alternating projection

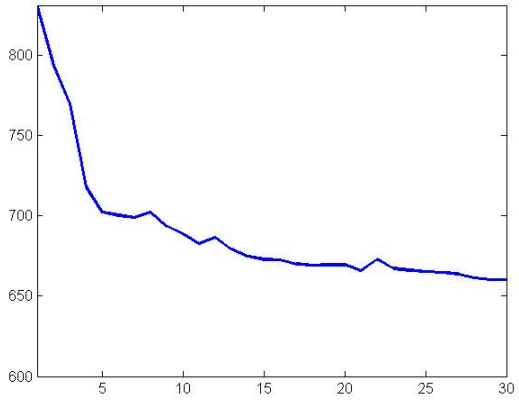

Fig. 5. MSE v.s iterations

[13] R. Tibshirani, "Regression shrinkage and selection via the lasso," *Journal of the Royal Statistical Society. Series B (Methodological)*, vol. 58, no. 1, pp. 267–288, 1996.

[14] M.A.T. Figueiredo, R.D. Nowak, and S.J. Wright, "Gradient projection for sparse reconstruction: Application to compressed sensing and other inverse problems," *Selected Topics in Signal Processing, IEEE Journal of*, vol. 1, no. 4, pp. 586–597, 2008.

[15] R.N. Bracewell, *Two-dimensional imaging*, Prentice-Hall, Inc. Upper Saddle River, NJ, USA, 1995.

[16] R.O. Duda, P.E. Hart, and D.G. Stork, *Pattern classification*, Citeseer, 2001.

[17] M. Grant, S. Boyd, and Y. Ye, "CVX: Matlab software for disciplined convex programming," *avialable at http://www. stanford. edu/boyd/cvx*, vol. 1.

[18] A.C. Kak and M. Slaney, "Principles of computerized tomographic imaging," 1988.

[19] E.Y. Sidky and X. Pan, "Image reconstruction in circular cone-beam computed tomography by constrained, total-variation minimization," *Physics in medicine and biology*, vol. 53, pp. 4777, 2008.

[20] P.H. Calamai and J.J. Moré, "Projected gradient methods for linearly constrained problems," *Mathematical Programming*, vol. 39, no. 1, pp. 93–116, 1987.

Algorithm 1 Exact Algorithm Description

1: Choose the allowable error δ in observed data and stop criterion ρ. Also select Δ, ϵ.

2: Define the maximal iteration number l_{max} and set the iteration number $l_{iter} = 0$. Initialize the boundary $\widetilde{k}^{\lambda^{(0)}}$ with upper bound S, each pixel belongs to every group $i \in G_\lambda$ and the weight $\mathbf{w}_i^{\lambda^{(0)}} = 1, \forall i = 1, \ldots, n.\ \lambda = 1, \ldots, M$.

3: Solve the reweighed l_1 norm linear programming

$$\left[\mathbf{u}^{1^{(l_{iter})}}, \ldots, \mathbf{u}^{M^{(l_{iter})}}\right] = \arg\min_{\mathbf{u}^\lambda} \sum_{\lambda=1}^{M} \left\| \mathbf{w}^{\lambda^{(l_{iter})}} .* \mathbf{u}^\lambda \right\|_1$$

$$\text{subject to} \quad \|\mathbf{y} - \mathbf{A}\mathbf{x}\|_2 \leq \delta$$
$$\mathbf{x} = \sum_{\lambda=1}^{M} \widetilde{k}^\lambda \cdot \mathbf{T}\mathbf{u}^\lambda$$
$$-\mathbf{1} \leq \mathbf{u}^\lambda \leq \mathbf{1}, \ \ 0 \leq \mathbf{x}_i \leq D(i)$$

4: Update the weights: for each $i = 1, \ldots, n.\ \lambda = 1, \ldots, M$

$$\mathbf{w}_i^{\lambda^{(l+1)}} = \frac{1}{|\mathbf{u}_i^{\lambda^{(l)}}| + \Delta}$$

5: Run the Gaussian Mixture Model (GMM) clustering on the support $\mathbf{x}$ to partition them into M clusters. With the mean c^λ and variance σ^λ, update the boundary for new feasible region by

$$k^\lambda \leftarrow k^\lambda - \gamma(\frac{1}{\sigma^\lambda})(k^\lambda - c^\lambda)$$

6: Update the boundary of each pixel by forward mapping of each group $\mathbf{z}^\lambda = \widetilde{k}^\lambda \cdot \mathbf{T}\mathbf{u}^\lambda$

$$i \in G_\lambda \quad \text{if} \quad z_i^\lambda \geq \epsilon$$
$$D(i) = \max_{i \in G_\lambda} \{\widetilde{k}^\lambda\}$$

7: Terminate the iteration if $\left\|\mathbf{x}^{(l)} - \mathbf{x}^{(l-1)}\right\|_2 \leq \rho$ or l_{iter} reaches the maximum number of iteration. Otherwise, increase l_{outer} and go to step 3.